

2008

Absorption Spectral Slopes and Slope Ratios as Indicators of Molecular Weight, Source, and Photobleaching of Chromophoric Dissolved Organic Matter

John R. Helms
Old Dominion University

Aron Stubbins
Old Dominion University


Jason D. Ritchie
Old Dominion University

Elizabeth C. Minor
Old Dominion University

David J. Kieber

See next page for additional authors

Follow this and additional works at: https://digitalcommons.odu.edu/chemistry_fac_pubs

 Part of the [Chemistry Commons](#), [Fresh Water Studies Commons](#), [Marine Biology Commons](#), and the [Oceanography Commons](#)

Repository Citation

Helms, John R.; Stubbins, Aron; Ritchie, Jason D.; Minor, Elizabeth C.; Kieber, David J.; and Mopper, Kenneth, "Absorption Spectral Slopes and Slope Ratios as Indicators of Molecular Weight, Source, and Photobleaching of Chromophoric Dissolved Organic Matter" (2008). *Chemistry & Biochemistry Faculty Publications*. 120.
https://digitalcommons.odu.edu/chemistry_fac_pubs/120

Original Publication Citation

Helms, J. R., Stubbins, A., Ritchie, J. D., Minor, E. C., Kieber, D. J., & Mopper, K. (2008). Absorption spectral slopes and slope ratios as indicators of molecular weight, source, and photobleaching of chromophoric dissolved organic matter. *Limnology and Oceanography*, 53(3), 955-969. doi:10.4319/lo.2008.53.3.0955

Authors

John R. Helms, Aron Stubbins, Jason D. Ritchie, Elizabeth C. Minor, David J. Kieber, and Kenneth Mopper

Absorption spectral slopes and slope ratios as indicators of molecular weight, source, and photobleaching of chromophoric dissolved organic matter

John R. Helms, Aron Stubbins, Jason D. Ritchie, and Elizabeth C. Minor¹

Department of Chemistry and Biochemistry, Old Dominion University, Norfolk, Virginia 23529

David J. Kieber

Chemistry Department, State University of New York, School of Environmental Science and Forestry, Syracuse, New York 13210

Kenneth Mopper²

Department of Chemistry and Biochemistry, Old Dominion University, Norfolk, Virginia 23529

Abstract

A new approach for parameterizing dissolved organic matter (DOM) ultraviolet-visible absorption spectra is presented. Two distinct spectral slope regions (275–295 nm and 350–400 nm) within log-transformed absorption spectra were used to compare DOM from contrasting water types, ranging from wetlands (Great Dismal Swamp and Suwannee River) to photobleached oceanic water (Atlantic Ocean). On the basis of DOM size-fractionation studies (ultrafiltration and gel filtration chromatography), the slope of the 275–295-nm region and the ratio of these slopes (S_R ; 275–295-nm slope:350–400-nm slope) were related to DOM molecular weight (MW) and to photochemically induced shifts in MW. Dark aerobic microbial alteration of chromophoric DOM (CDOM) resulted in spectral slope changes opposite of those caused by photochemistry. Along an axial transect in the Delaware Estuary, large variations in S_R were measured, probably due to mixing, photodegradation, and microbial alteration of CDOM as terrestrially derived DOM transited through the estuary. Further, S_R varied by over a factor of 13 between DOM-rich wetland waters and Sargasso Sea surface waters. Currently, there is no consensus on a wavelength range for log-transformed absorption spectra. We propose that the 275–295-nm slope be routinely reported in future DOM studies, as it can be measured with high precision, it facilitates comparison among dissimilar water types including CDOM-rich wetland and CDOM-poor marine waters, and it appears to be a good proxy for DOM MW.

The properties of dissolved organic matter (DOM) are diverse and depend on its source (e.g., terrestrial vs. aquatic) and diagenetic state. The fraction of DOM that absorbs ultraviolet (UV) and visible light is referred to as chromophoric or colored dissolved organic matter (CDOM). CDOM is largely responsible for the optical properties of most natural waters and plays key roles in shielding biota from harmful UV radiation (Walsh et al. 2003) and in several biogeochemical and photochemical processes (e.g., Mopper and Kieber 2002).

UV-visible absorption spectra for CDOM increase approximately exponentially with decreasing wavelength (Twardowski et al. 2004). To extract information from these spectra about CDOM properties, several spectral parameters, primarily absorption ratios, have been defined. These ratios are largely independent of CDOM concentration, which is important in regimes such as estuaries, where CDOM concentrations often vary by a factor of five or more. De Haan and De Boer (1987) used the ratio of absorption at 250 to 365 nm (called $E_2:E_3$) to track changes in the relative size of DOM molecules (see also Peuravouri and Pihlaja 1997). As molecular size increased, $E_2:E_3$ decreased because of stronger light absorption by high-molecular-weight (HMW) CDOM at longer wavelengths. The ratio of absorption at 465 to 665 nm ($E_4:E_6$) was reported to be inversely related to CDOM aromaticity (Summers et al. 1987; Piccolo et al. 1992; Chin et al. 1994). However, $E_4:E_6$ ratios have been shown to be better correlated with molecular size, O:C and C:N atom ratios, carboxyl content, and total acidity than to aromaticity (Chen et al. 1977; Senesi et al. 1989) and, therefore, may be better suited as a general tracer of humification. In many natural waters (as opposed to XAD resin extracts and soil extracts), where there is often little or no measurable absorption at 665 nm, absorption at 254 nm (or sometimes 280 nm) has been used in lieu of the $E_4:E_6$ ratio as an indicator of humification or aromaticity (Summers et al.

¹Present address: Large Lakes Observatory, University of Minnesota Duluth, Duluth, Minnesota 55812.

²Corresponding author.

Acknowledgments

We thank Tim Brown, Brent Dalzell, Hussain Abdulla, Nianhong Chen, and Joy Davis for UV-visible and DOC measurements as well as ultrafiltration of Elizabeth River and Chesapeake Bay samples. We thank E. M. Perdue for providing the SEC data, and George Westby and the crew of the RV *Endeavor* for their assistance in collecting samples and data in the Delaware Estuary. We acknowledge Robert F. Dias and two anonymous reviewers for their helpful comments.

This research was supported by the following NSF grants: OCE-0096426, OCE-0096413, OCE-0241946, OCE-0327423, OCE-0555245, and OPP-0230499.

1987; Weishaar et al. 2003). Weishaar et al. (2003) showed that UV absorption at 254 nm, when normalized to dissolved organic carbon (DOC) concentration, a parameter called specific UV absorbance (SUVA₂₅₄), correlated strongly ($r^2 > 0.97$) with DOM aromaticity, as determined by ¹³C-nuclear magnetic resonance (¹³C-NMR), for a large number of humic substance isolates.

In addition to the above parameters, the spectral slope (S , nm⁻¹) has been derived from CDOM absorption spectra by fitting the absorption data to the equation:

$$a_{\lambda} = a_{\lambda_{\text{ref}}} e^{-S(\lambda - \lambda_{\text{ref}})} \quad (1)$$

where a = Napierian absorption coefficient (m⁻¹), λ = wavelength (nm), and λ_{ref} = reference wavelength (nm) (e.g., Twardowski et al. 2004).

Spectral slopes provide further insights into the average characteristics (chemistry, source, diagenesis) of CDOM than absorption values alone, and like the $E_2:E_3$ and $E_4:E_6$ ratios, they are largely independent of CDOM concentration (Brown 1977). S has been used for correcting remote sensing (bio-optic) data (Schwarz et al. 2002) and monitoring CDOM degradative processes (Vähätalo and Wetzel 2004). Carder et al. (1989) showed that S may be used to semiquantitatively describe the ratio of fulvic acids (FA) to humic acids (HA) in a sample. Similarly, it was noted that S correlates strongly with molecular weight (MW) of isolates of fulvic acids but not humic acids (Hayase and Tsubota 1985; Carder et al. 1989).

From the above, it is apparent that S is potentially useful for characterizing DOM. However, its usefulness is limited by the fact that the value obtained for S depends on the wavelength interval over which it is calculated (Carder et al. 1989; Stedmon et al. 2000). In fact, using a narrow wavelength range to calculate S often provides a different result from that obtained with a broader range (Twardowski et al. 2004). The use of narrow wavelength intervals is advantageous as they minimize variations in S caused by dilution (Brown 1977). Sarpal et al. (1995) found that the slopes of two narrow wavelength intervals, 260–330 nm and 330–410 nm, described log-transformed absorption spectra of seawater (Antarctic waters) far better than a single slope determined over a broader wavelength interval. Further, these investigators suggested that the use of S over narrow spectral regions may be exploited to reveal subtle differences in the shape of spectra, which, in turn, may provide compositional or diagenetic insights.

In addition to the wavelength range chosen, the value obtained for S also depends on the method used for its calculation. For example, Stedmon et al. (2000) and Del Vecchio and Blough (2004a) demonstrated that spectra are often better described by nonlinear regression fitting routines, especially over broad wavelength ranges and where absorption approaches the detection limit of the instrument. As a result of the lack of a standardized mathematical or operational definition of S (i.e., linear vs. nonlinear regression) or a specific wavelength range for its calculation, the literature contains a wide range in values for S even for similar sample types (for a review see Twardowski et al. 2004). This lack of standardization has

made comparisons of published S values difficult or impossible, and, in fact, has resulted in contradictory conclusions. For example, Miller (1994), Morris and Hargraeves (1997), and Gao and Zepp (1998) reported that S decreased during irradiation of natural water samples, which runs counter to the findings of several other studies (e.g., Whitehead et al. 2000; Del Vecchio and Blough 2002; Vähätalo and Wetzel 2004). However, the apparent contradictory results were internally consistent given the wavelength ranges and fitting routines that were chosen.

Like the $E_2:E_3$ ratio, the spectral slope has been used as a proxy for MW in a broad range of samples. However, S has only been shown to covary with MW for CDOM that was isolated by solid-phase extraction (e.g., XAD resins or C-18 silica) or fractionated in relatively harsh acid–base conditions (Zepp and Schlotzhauer 1981; Hayase and Tsubota 1985; Carder et al. 1989). Consequently, observed differences in MW between FA and HA fractions, to some extent, may have resulted from artifacts related to the isolation methods (Schmit and Wells 2002).

In this study, these potential artifacts and the dependence of S on wavelength range are addressed by examining absorption spectra of sterile-filtered whole water, ultrafiltered samples (~1-kDa permeates and retentates), and gel filtration chromatography (GFC) size fractions; and by determining S over two narrow wavelength ranges. By calculating the ratio of the slope of the shorter wavelength region (275–295 nm) to that of the longer wavelength region (350–400 nm), a dimensionless parameter called “slope ratio” or S_R is defined. This approach avoids the use of spectral data near the detection limit of the instruments used, and focuses on absorbance values that shift dramatically during estuarine transit and photochemical alteration of CDOM. We investigate here the dependence of spectral shape parameters (primarily S and S_R) on the MW distribution of aquatic CDOM samples from a broad range of environments.

Methods and materials

Cleaning procedures—All glassware was cleaned with dilute (5–10%) HCl and rinsed with MilliQ ultrapure-grade water (Millipore). Glassware was either combusted at 450°C or autoclaved before use. Plasticware was cleaned with 5–10% HCl and rinsed with MilliQ water. Stainless steel equipment was cleaned with mild detergent and copiously rinsed with MilliQ. All containers were rinsed several times with sample before filling. Filter capsules (0.1 μm or 0.2 μm pore size, Whatman PolyCap) were rinsed with acetonitrile, flushed with >20 liters of MilliQ water, and conditioned with approximately 1 liter of sample.

Elizabeth River, Great Dismal Swamp, and lower Chesapeake Bay—Water samples were taken from three sites within the Elizabeth River and Chesapeake Bay estuary system during May 2004, October 2004, May 2005, and October 2005. The Elizabeth River estuary is tidally influenced over its entire length and receives

substantial input of CDOM-rich water from the Great Dismal Swamp canal system (by way of the Deep Creek Lock, Portsmouth Ditch, and several other small creeks). At our sampling times, the salinity at the upriver site ranged between 8 and 12 and contained high concentrations of DOC (typically 10–20 mg L⁻¹). Our high-salinity (marine) station (the mouth of the Chesapeake Bay; salinity = 23–26) is at the confluence of several estuarine systems (typical DOC concentrations were 1–2 mg L⁻¹).

Sampling was always performed at low tide using a stainless steel or polypropylene bucket. The samples were transported in polypropylene carboys back to the lab, where they were gravity filtered using high-flow filter capsules within 12 h of collection. The filtrate was collected and stored in a glass carboy, which was wrapped in black plastic to minimize light exposure. The filtered water samples were placed in 500-mL round-bottom quartz glass flasks and irradiated using the solar simulator described below. In 2004, UV-visible absorption spectra (200–800 nm) were measured for irradiated samples and dark controls using a double-beam scanning spectrophotometer (Bio300 UV-Vis Cary, Varian) with 1-cm quartz cuvettes and ultrapure water (Elga) as the blank. In May 2005, measurements were made using a Hitachi U-1000 double-beam spectrophotometer with either 1-cm or 10-cm quartz cuvettes and ultrapure water (Elga) as the blank. In October 2005, spectra were taken with an Agilent 8453 diode array spectrophotometer using either a 1-cm or 5-cm quartz cuvette.

Irradiated and dark control 0.1- μ m- or 0.2- μ m-filtered samples were also size fractionated by ultrafiltration (UF) using Amicon 8400 stirred cells fitted with 1,000-Da regenerated cellulose membranes (Millipore YM1, 76-mm diameter) and pressurized using ultrapure nitrogen. Sterile filtered (non-UF fractionated) samples, UF permeates, and retentates were analyzed by high-temperature combustion DOC analysis (Shimadzu TC-5000) to measure the non-purgeable organic carbon concentration and by UV-visible spectroscopy to measure absorption spectra as described above. UV-visible mass balances were calculated using the total (volume-corrected) absorption integrated from 250 to 450 nm and are presented as a percentage of the absorption measured for the two size fractions (i.e., permeate and retentate) divided by the absorption measured for the non-UF sample. DOC mass balances were calculated from the concentration of DOC (measured via high-temperature combustion on acidified samples) for both size fractions (volume corrected) divided by the DOC concentration of the non-UF sample.

In June 2004 and February 2006, samples were collected from the Portsmouth Ditch and Northwest Canal sections, respectively, of the Great Dismal Swamp canal system. Samples were collected and filtered as above. The Northwest Canal sample was irradiated using the solar simulator described below and ultrafiltered as described above. One aliquot of the sample was sparged with ultrapure helium to significantly decrease the concentration of dissolved molecular oxygen during light exposure. Before UV-visible absorption measurement, samples were diluted by a factor of five in MilliQ water to bring the

absorbance into the linear response range of the spectrophotometer (1-cm pathlength).

In July 2005 the Old Dominion University (ODU) Sailing Basin site on the Elizabeth River (salinity = 19) was sampled to investigate microbial (community) effects on the shape of the CDOM UV-visible spectrum. The unfiltered, unamended water sample was stirred constantly, kept at room temperature, in the dark, and maintained at equilibrium with lab air for 2 weeks. Duplicate 20-mL subsamples were collected at intervals and immediately poisoned with 100 μ mol L⁻¹ potassium cyanide (final concentration). Samples were allowed to settle for at least 7 d, after which they were analyzed using the Agilent 8453 spectrophotometer with a 1-cm quartz cell. Blanks consisting of an exact aliquot of poison in MilliQ water were prepared at the time of each poisoning.

Suwannee River natural organic matter (SRNOM)—A well-characterized aquatic humic substance sample was separated by size using preparative gel filtration chromatography (GFC) according to the procedure in Ritchie (2005). Briefly, 1 g of SRNOM (International Humic Substances Society, 1R101N) was separated into six size fractions on a column packed with Superdex-30 (Amersham Pharmacia Biotech-GE Healthcare) that was calibrated using polystyrene sulfonate salts (Polysciences), methylthymol blue, and *p*-hydroxybenzoic acid. The mobile phase consisted of a NaHCO₃/Na₂CO₃ mixture (pH = 9.2, ionic strength = 0.1 mol L⁻¹). Size fraction 1 (greatest apparent MW) through fraction 6 (smallest apparent MW) represent fractions collected sequentially from the Gaussian-like hump between the total permeation volume and total exclusion volume of the column. Each size fraction was subsequently desalted and freeze dried. The average MW of each size fraction was determined by analytical size-exclusion chromatography (SEC). SEC was performed using Superdex-30 stationary phase packed in a 0.6-cm-diameter Pharmacia column with UV detection at 254 nm. The mobile phase consisted of 0.1 mol L⁻¹ NaCl buffered with 2 mmol L⁻¹ phosphate adjusted to pH 6.8 (1 mL min⁻¹). The GFC fractions and whole SRNOM were prepared at 15 mg C L⁻¹ with the same electrolyte concentrations as the mobile phase, and polystyrene sulfonate salts were used as MW standards. For UV-visible absorbance measurements, the size fractions were prepared as for SEC. Spectra were recorded using a 1-cm quartz cuvette at 25°C on a HP 8451 diode array spectrophotometer with 2-nm resolution.

Delaware Estuary and Atlantic Ocean—Surface water samples were collected during two transects along the main axis of the Delaware Estuary in the summers of 2000 and 2002 on board the RV *Endeavor* and again in the summer of 2005 aboard the RV *Cape Henlopen*, from the ships' clean seawater supply systems, which were fed from an inlet at ~2–3-m depth. Surface samples in the coastal waters near the mouth of the bay and along the mid-Atlantic Bight were also obtained from the underway system. In a third *Endeavor* cruise during summer 2003, waters were sampled at two coastal sites in the Georgia Bight (GAB). Samples were collected at depths from 4 to 10 m using 20-liter GO-

FLO™ bottles. All water samples were filtered and stored as described above. The UV-visible measurements were made at sea using a Hewlett Packard 8453 diode array spectrophotometer equipped with a 5-cm flow cell with MilliQ water as the blank.

Samples from the near-shore GAB sample site, Sta. B, were exposed to sunlight on the ship's deck, as well as in a shipboard solar simulator containing three UVA340 (Q-Panel) bulbs and three full-spectrum fluorescent bulbs (GE Spectra Rays F40T12/SR). Sample UV-visible absorption spectra were measured onboard using the Hewlett Packard 8453 spectrophotometer, as described above.

In June 2006, surface waters were collected from the Delaware River at the Yardley, Pennsylvania public boat ramp by completely submerging several precleaned polypropylene carboys. Samples were 0.1 μm filtered and poisoned with mercuric chloride (0.1 mL saturated solution per liter of sample) to inhibit microbial regrowth. Control experiments showed that mercuric chloride had no discernable effect on either photoreactivity or UV-visible spectra. Samples were exposed to sunlight for 3 weeks in August on the roof of the chemistry building on the campus of ODU in Norfolk, Virginia. The containers used during the irradiation were 80-liter polycarbonate tubs (Rubbermaid) with lids modified to include UV-transparent fluorinated ethylene-propylene windows (American Durafilm). Subsamples were collected at 2- to 4-d intervals using clean silicon tubing and analyzed using the Agilent 8453 diode array spectrophotometer.

Sample irradiation system—Unless indicated otherwise, both light-exposed samples and dark controls were placed on a rotating table (1 revolution per minute) within a solar simulator containing 12 Q-Panel UV340 bulbs, which provided a spectral shape similar to that of natural sunlight from ~ 295 to ~ 365 nm (Q-Panel), but underrepresented solar radiation at wavelengths greater than about 365 nm. The light output from the solar simulator was measured using an International Light IL-1700 radiometer, equipped with an SUD240 sensor and a W#6931/300#14571 filter/diffuser (UVA), and was comparable with springtime, noon sunlight intensity at 40°N (Leifer 1988). To directly compare our irradiations with sunlight, an Elizabeth River water sample was irradiated for 5 h under both natural and simulated sunlight, and the extent of photobleaching (integrated over 250 to 400 nm) was determined. In this comparison, the solar simulator provided 127% of the photobleaching occurring under winter midday sunlight at 36.89°N .

Spectral corrections and S determination—CDOM absorbance was assumed to be zero above 700 nm; therefore, the average sample absorbance between 700 and 800 nm was subtracted from the spectrum to correct for offsets due to instrument baseline drift, temperature, scattering, and refractive effects (Green and Blough 1994). Absorbance units were converted to absorption coefficients as follows:

$$a = 2.303A/l \quad (2)$$

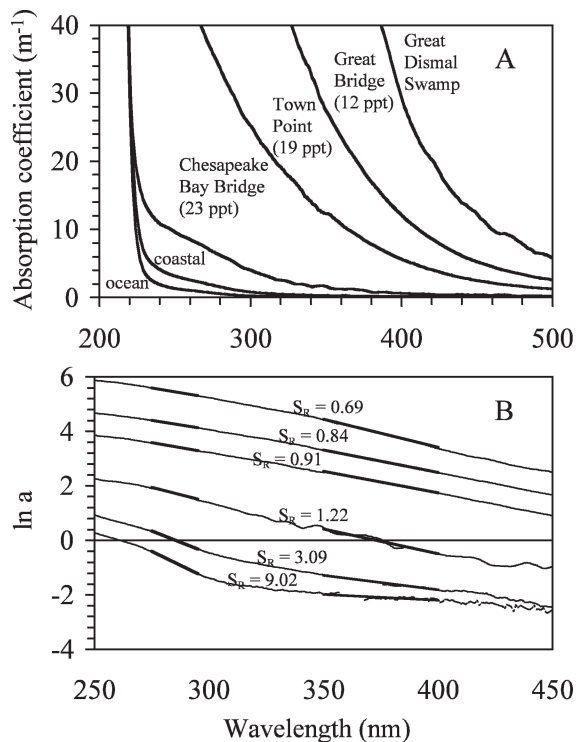


Fig. 1. (A) Absorption spectra obtained for 0.2 μm filtered water samples from six sites: Great Dismal Swamp, Great Bridge and Town Point in the Elizabeth River estuary, Chesapeake Bay Bridge on the lower Chesapeake Bay (all collected in spring 2004), a coastal site on the Georgia Bight (coastal), and Sargasso Sea (ocean). (B) Natural log-transformed absorption spectra for the above samples with best-fit regression lines for two regions (275–295 nm and 350–400 nm); slope ratio (S_R) values are given for each log-transformed spectrum.

where a = absorption coefficient (m^{-1}), A = absorbance, and l = path length (m).

The spectral slope for the interval of 300–700 nm ($S_{300-700}$) was determined by fitting the absorption spectra to a single exponential decay function (Eq. 1) by nonlinear regression (SigmaPlot). Spectral slopes reported here for the intervals of 275–295 nm ($S_{275-295}$) and 350–400 nm ($S_{350-400}$) were calculated using linear regression of the log-transformed a spectra. $S_{275-295}$ and $S_{350-400}$ were calculated, for a subset of sample spectra, using both the log-transform linear regression and nonlinear regression methods. Variation between the two methods was less than 1%. Slopes are reported as positive numbers to follow the mathematical convention of fitting to an exponential decay (Eq. 1). Thus, higher (or steeper) slopes indicate a more rapid decrease in absorption with increasing wavelength. The ranges, 275–295 nm and 350–400 nm, were chosen because the first derivative of natural-log spectra indicated that the greatest variations in S from a variety of samples (marsh, riverine, estuarine, coastal, and open ocean) occurred within the narrow bands of 275–295 nm and 350–400 nm. The slope ratio or S_R was calculated as the ratio of $S_{275-295}$ to $S_{350-400}$. The $E_2:E_3$ and $E_4:E_6$ ratios were calculated using absorption coefficients at the appropriate wavelengths. SUVA₂₅₄ was calculated by

Table 1. Mass balances on the basis of total absorption (250–450 nm) and dissolved organic carbon measurements for each of the ultrafiltration size fractions. Chesapeake Bay Bridge (CBB), Town Point (TP), Great Bridge (GB), and Dismal Swamp (DS); init=initial; con=dark control; T1=irradiated 24 h; T2= irradiated 48 h; ox=air saturated; anox=He sparged, low oxygen samples.

	Sample name	Salinity	Irr <i>t</i> (h)	%LMW CDOM	%HMW CDOM	%CDOM recovery	%LMW DOC	%HMW DOC	%DOC recovery
May 2004	GB init	12	0	18.9	72.9	91.8	41.7	68.2	109.9
May 2004	GB con	12	0	16.5	74.5	91.0	39.2	71.0	110.2
May 2004	GB T1	12	24	22.8	72.4	95.2	40.9	60.6	101.5
May 2004	GB T2	12	48	22.2	65.7	87.9	31.5	54.6	86.1
May 2004	TP init	19	0	29.8	67.6	97.4	49.7	61.8	111.5
May 2004	TP con	19	0	25.3	65.0	90.3	43.5	56.3	99.8
May 2004	TP T1	19	24	36.0	65.2	101.1	63.0	62.4	125.4
May 2004	TP T2	19	48	41.3	52.3	93.6	62.3	54.6	116.9
May 2004	CBB init	23	0	57.4	43.9	101.3	59.1	38.5	97.6
May 2004	CBB con	23	0	49.8	51.6	101.4	54.9	47.2	102.1
May 2004	CBB T1	23	24	70.7	47.9	118.6	67.3	48.2	115.5
May 2004	CBB T2	23	48	60.0	40.6	100.6	51.1	35.5	89.6
Oct 2004	GB init	10	0	17.5	89.4	106.9	26.0	67.6	93.6
Oct 2004	GB con	10	0	19.6	77.1	96.7	31.0	69.3	100.3
Oct 2004	GB T1	10	24	30.3	78.8	109.1	33.6	59.2	92.8
Oct 2004	GB T2	10	48	26.4	74.4	100.8	57.7	59.1	116.8
Oct 2004	TP init	17	0	24.4	70.6	95.0	36.1	59.2	95.3
Oct 2004	TP con	17	0	24.3	78.5	102.8	38.8	62.1	100.9
Oct 2004	TP T1	17	24	32.1	67.7	99.8	37.2	52.4	89.6
Oct 2004	TP T2	17	48	31.4	57.4	88.8	49.0	47.0	96.0
Oct 2004	CBB init	26	0	35.1	78.3	113.4	88.0	35.2	123.3
Oct 2004	CBB con	26	0	18.4	51.8	70.2	70.9	20.8	91.7
Oct 2004	CBB T1	26	24	No data	No data	No data	61.7	27.9	89.6
Oct 2004	CBB T2	26	48	No data	No data	No data	82.5	24.0	106.5
May 2005	GB init	8	0	26.8	65.7	92.5	40.5	60.5	101.0
May 2005	GB con	8	0	29.1	65.4	94.5	43.2	63.4	106.6
May 2005	GB T1	8	24	29.7	79.9	109.6	66.4	56.1	122.5
May 2005	GB T2	8	48	32.3	58.7	91.0	46.1	48.0	94.0
May 2005	TP init	18	0	22.5	71.4	93.9	36.3	51.3	87.6
May 2005	TP con	18	0	24.6	73.6	98.3	45.4	60.7	106.2
May 2005	TP T1	18	24	36.9	55.5	92.4	60.5	51.6	112.1
May 2005	TP T2	18	48	38.5	63.0	101.5	103.8	45.9	149.7
May 2005	CBB init	25	0	46.0	No data	No data	55.6	22.8	78.5
May 2005	CBB con	25	0	45.9	No data	No data	52.1	20.9	73.1
May 2005	CBB T1	25	24	43.7	No data	No data	No data	No data	No data
May 2005	CBB T2	25	48	45.0	No data	No data	64.5	17.9	82.5
Oct 2005	GB init	11	0	19.3	71.6	90.8	No data	No data	No data
Oct 2005	GB con	11	0	21.5	73.2	94.6	No data	No data	No data
Oct 2005	GB T1	11	24	25.3	67.0	92.3	No data	No data	No data
Oct 2005	GB T2	11	48	27.6	60.8	88.4	No data	No data	No data
Oct 2005	TP init	18	0	23.4	67.3	90.7	No data	No data	No data
Oct 2005	TP con	18	0	23.5	62.0	85.5	No data	No data	No data
Oct 2005	TP T1	18	24	28.4	63.9	92.3	No data	No data	No data
Oct 2005	TP T2	18	48	34.2	55.3	89.5	No data	No data	No data
Oct 2005	CBB init	23	0	49.4	54.8	104.2	No data	No data	No data
Oct 2005	CBB con	23	0	No data	31.8	No data	No data	No data	No data
Oct 2005	CBB T1	23	24	60.3	40.6	110.9	No data	No data	No data
Oct 2005	CBB T2	23	48	68.4	37.6	106.0	No data	No data	No data
Feb 2006	DS ox con	0	0	9.4	88.7	98.1	No data	No data	No data
Feb 2006	DS ox T1	0	144	24.3	77.3	101.6	No data	No data	No data
Feb 2006	DS anox con	0	0	7.5	88.0	95.5	No data	No data	No data
Feb 2006	DS anox T1	0	144	12.0	85.6	97.6	No data	No data	No data

dividing a_{254} (m^{-1}) by the DOC concentration (mg L^{-1}) as in Weishaar et al. (2003). The total CDOM absorption was calculated as the integrated absorption from 250 to 450 nm (1-nm resolution).

Results

MW and spectral shape—Figure 1A shows absorption spectra obtained for a variety of freshwater, estuarine, and

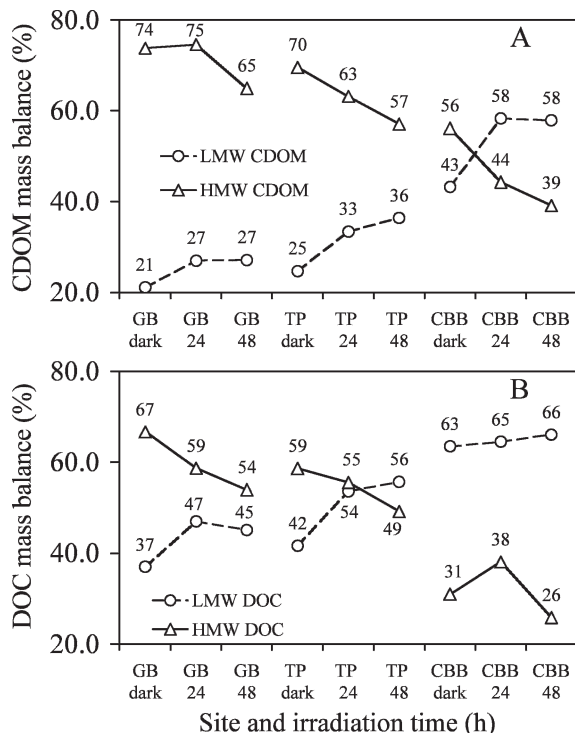


Fig. 2. (A) CDOM and (B) DOC mass balance percentages averaged over all four sampling seasons. Great Bridge (GB), Town Point (TP), and Chesapeake Bay Bridge (CBB); Dark, dark control (no irradiation); 24, irradiated for 24 h; 48, irradiated for 48 h. Percentages are given above each symbol.

marine samples. Figure 1B illustrates the linearization and least-squares fit of these spectra, with the linear fit shown for the spectral regions 275–295 nm and 350–400 nm. There are visible distinctions between the slopes for these two regions, depending on whether the sample is mainly terrestrial or marine in character; e.g., for marine samples $S_{275-295} > S_{350-400}$, whereas the opposite trend holds for high-CDOM, terrestrially dominated samples.

Absorption and DOC mass balances for the ultrafiltered Elizabeth River samples are given in Table 1 and Fig. 2. These results show two general trends. First, the lower-salinity upriver samples contained more HMW CDOM (>1,000 Da) relative to low-MW (LMW) CDOM (<1,000 Da) than the high-salinity Chesapeake Bay samples. Second, the percentage of CDOM in the LMW fraction in all three sampling sites increased upon light exposure, whereas in the HMW fraction, it decreased. The latter trend is especially pronounced for the upriver samples (Fig. 2; Table 1). These results indicate that there is a shift from HMW to LMW CDOM both with irradiation and with increasing salinity across the freshwater–marine continuum.

The UV-visible absorption (a), spectral slope (S), and slope ratio (S_R) obtained for the 0.2- μm -filtered samples showed several consistent trends. Upriver samples had higher absorption coefficients (Fig. 1), lower $S_{275-295}$ values, and lower S_R values (Figs. 3, 4; Table 2) than downriver and Chesapeake Bay samples. Irradiation

consistently increased $S_{275-295}$, S_R , and $E_2:E_3$, and decreased UV absorption and DOC (Figs. 3, 4; Table 2) for samples from all three sites (e.g., compare the four samples from any single site in Table 2). Furthermore, $S_{275-295}$ and S_R values of the HMW (>1,000-Da UF retentate) fractions were generally lower than those for the corresponding LMW (UF permeate) fractions (Table 3). In addition, spectral slopes $S_{275-295}$ and $S_{350-400}$ for both MW fractions showed consistent shifts upon irradiation, with $S_{275-295}$ generally increasing upon irradiation and $S_{350-400}$ values generally decreasing (e.g., compare treatments from a single site and season in Table 3). These results provide evidence that shifts in S_R and $S_{275-295}$ are related to shifts in MW and photobleaching. Figure 4A shows that S_R correlates well with CDOM MW, as determined from the UF experiments. In this figure, S_R values of 0.2- μm -filtered samples were plotted against the ratio of LMW to HMW absorption (integrated over 250–450 nm), whereas Fig. 4B shows the plot on a DOC basis. The S_R values correlated with MW shifts in the estuary (i.e., for dark controls and initial samples) and with shifts in MW that occurred during the 48-h irradiations on both a CDOM and DOC basis. The latter implies that estimates of MW on the basis of CDOM measurements likely apply to total DOM. The $E_2:E_3$ ratio (Table 2) also showed a linear correlation with MW in irradiated samples. However, this correlation was less robust (Helms 2006) and was generally not applicable to marine waters where 365-nm CDOM absorption often approached the detection limit of traditional spectrophotometers with 10-cm quartz cuvettes (Stubbins 2006).

In agreement with the above Elizabeth River–Chesapeake Bay results, we found that the spectral slopes of size-fractionated SRNOM were highly correlated to weight-average MW over the size range analyzed (Fig. 5A,B), whereas the S_R parameter (Fig. 5C) was only linearly related to MW less than 3,000 Da. In each plot, the unfractionated SRNOM sample plotted near the scatter of the size-fractionated results. Using broader wavelength ranges such as 300–700 nm (data not shown) also yielded linear trends (slope = $1.81 \times 10^{-6} \text{ nm}^{-1} \text{ Da}^{-1}$; $r^2 = 0.903$).

Long-term (6 d) irradiation of the Dismal Swamp samples caused significant decreases in overall CDOM absorption and a large transfer of colored material from the HMW fraction to the LMW fraction (Tables 1, 3), whose absolute absorption actually increased. S_R increased from a terrestrial value (~ 0.71) to one more typical of estuarine or coastal samples (~ 1.1) (Table 2). Partial removal of oxygen (initial oxygen concentration reduced to 21% saturation, resulting in 88% less photochemical oxygen consumption than in oxygenated samples) before the irradiation of the Dismal Swamp samples decreased the extent to which CDOM was photobleached (Table 2), as well as the extent to which CDOM shifted from HMW to LMW pool (Tables 1, 3). However, this partial removal of oxygen did not significantly affect the light-induced shift in S and S_R for this sample (Table 2). This anomalous result will be discussed below.

Interestingly, changes in spectral shape (and consequently S and S_R values) caused by microbial activity differed significantly from those observed for photochemical

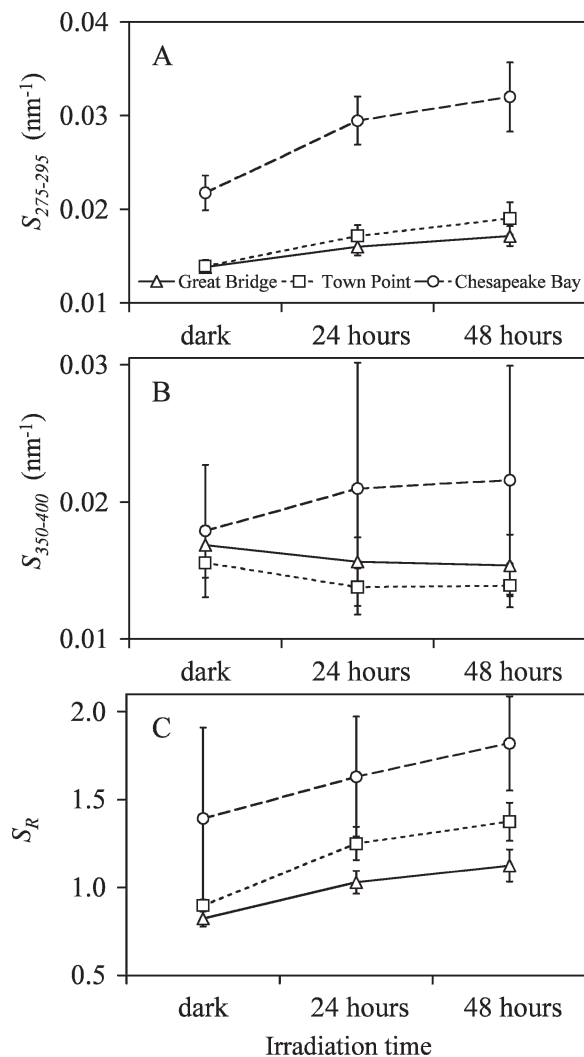


Fig. 3. Spectral slope parameters averaged over all four sampling seasons. (A) $S_{275-295}$, (B) $S_{350-400}$, and (C) ratio of spectral slopes, S_R , increase down-estuary and with increasing irradiation dose during an experiment. The vertical bars represent seasonal and interannual variations, not analytical error (analytical error was usually <1%).

degradation. Aerobic microbial incubations in the dark resulted in a statistically significant decrease in S_R over timescales of days to weeks (from $S_R = 1.02$ to $S_R = 0.94$ in 2 weeks) (Fig. 6), either due to the microbial production or selective preservation of long-wavelength-absorbing substances. This result is consistent with previous studies that found that microbial processes shifted spectral slopes opposite, but of a lower magnitude, to those caused by photochemistry over timescales of several weeks to several months (Moran et al. 2000; Vähätalo and Wetzel 2004). Our results therefore indicate that the down-estuary changes in optical properties are likely the result of a combination of processes, including mixing of low- S_R freshwater with high- S_R marine water, photochemically induced increases in S_R values, and microbially related decreases in S_R values.

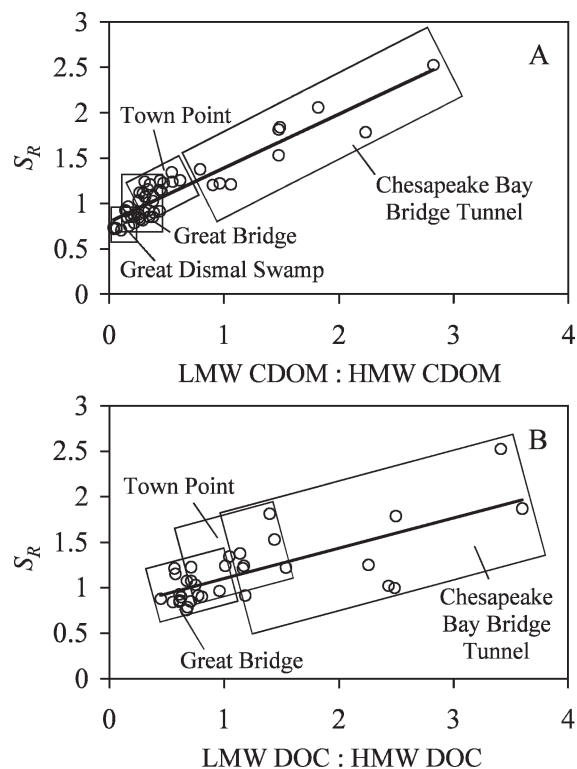


Fig. 4. Regression plots of the ratio of spectral slopes (S_R) versus molecular weight distribution, quantified by (A) UV-visible absorption and by (B) DOC concentration, for samples from the Great Dismal Swamp (absorbance data only), Elizabeth River (Town Point, Great Bridge), and Chesapeake Bay Bridge Tunnel, as delineated by the boxes. S_R values were based on unfracti-onated samples, whereas MW fractions were calculated independently of these spectra (see Methods and materials). (A) Slope = 0.594, intercept = 0.794, $r^2 = 0.858$; (B) slope = 0.333, intercept = 0.7663, $r^2 = 0.531$.

Spectral changes in the Delaware Estuary— S_R values within the Delaware estuary ranged from 0.88 in the river to 1.32 at the bay mouth. Figure 7C illustrates that S_R showed remarkably similar trends with salinity in summer 2000, 2002, and 2005. These trends were likely primarily due to mixing of river water with marine water in the estuary, and to progressive photobleaching during the downstream transit, especially near the mouth of the bay. Figure 8 shows that $S_{275-295}$ and S_R values throughout the estuary are somewhat higher than would be predicted by simple two end-member mixing, whereas $S_{350-400}$ values are lower than predicted by mixing. These deviations are most likely due to photochemical bleaching of CDOM, as inputs of marsh- (i.e., terrestrially) derived DOM in the lower estuary would have resulted in opposite deviations (Fig. 1).

The down-estuary increase in S_R was mainly due to an increase in $S_{275-295}$ (Fig. 7A, 8A), which is much more sensitive to DOM spectral changes within the estuary than $S_{300-700}$ (Fig. 7A). However, the sensitivity of S_R as an indicative parameter is enhanced by the decrease of slope in the long-wavelength region (Fig. 7A, 8B).

Irradiating surface water collected in the Delaware River with sunlight caused changes in S that were similar in

Table 2. Spectral parameters measured for each of the cartridge-filtered (<0.2 or <0.1 μm) samples from the Chesapeake Bay Bridge (CBB), Town Point (TP), Great Bridge (GB), and Dismal Swamp (DS); init=initial; con=dark control; T1=irradiated 24 h; T2=48 h.

Sample name	Salinity	Irr t (h)	S ₃₀₀₋₇₀₀ (nm ⁻¹)	S ₂₇₅₋₂₉₅ (nm ⁻¹)	S ₃₅₀₋₄₀₀ (nm ⁻¹)	S _R	Total a (250-450 nm)	DOC (mmol L ⁻¹)	E ₂ :E ₃	a ₂₅₄ (m ⁻¹)	a ₃₀₀ (m ⁻¹)	SUVA ₂₅₄ (mg C L ⁻¹ m ⁻¹)
May 2004 GB init	12	0	0.0157	0.0144	0.0167	0.859	7,094	820	5.00	102.7	57.2	10.40
May 2004 GB con	12	0	0.0158	0.0139	0.0165	0.841	7,171	857	4.97	103.1	58.7	10.00
May 2004 GB T1	12	24	0.0153	0.0165	0.0153	1.08	6,007	859	5.42	91.0	48.0	8.84
May 2004 GB T2	12	48	0.0154	0.0175	0.0151	1.15	5,204	911	5.88	82.8	41.1	7.59
May 2004 TP init	19	0	0.0150	0.0145	0.0161	0.901	3,171	428	4.80	45.7	25.5	8.91
May 2004 TP con	19	0	0.0149	0.0146	0.0160	0.914	3,126	407	4.85	45.1	25.6	9.24
May 2004 TP T1	19	24	0.0147	0.0186	0.0150	1.24	2,469	399	5.71	38.9	28.8	8.13
May 2004 TP T2	19	48	0.0146	0.0207	0.0150	1.38	2,052	390	6.23	34.5	25.7	7.39
May 2004 CBB init	23	0	0.0174	0.0191	0.0156	1.22	542	191	8.07	9.4	4.0	4.11
May 2004 CBB con	23	0	0.0174	0.0216	0.0178	1.21	509	192	7.71	9.0	4.5	3.94
May 2004 CBB T1	23	24	0.0149	0.0310	0.0171	1.81	370	177	8.74	7.3	2.8	3.47
May 2004 CBB T2	23	48	0.0170	0.0308	0.0201	1.53	315	224	10.74	6.8	2.2	2.56
Oct 2004 GB init	10	0	0.0146	0.0131	0.0155	0.845	10,264	1279	4.56	143.2	83.0	9.33
Oct 2004 GB con	10	0	0.0141	0.0131	0.0149	0.879	10,679	1237	4.51	148.9	85.8	10.00
Oct 2004 GB T1	10	24	0.0139	0.0150	0.0139	1.08	9,138	1216	4.83	133.2	71.8	9.13
Oct 2004 GB T2	10	48	0.0132	0.0163	0.0134	1.21	8,030	1106	5.13	121.9	62.5	9.19
Oct 2004 TP init	17	0	0.0130	0.0130	0.0140	0.926	6,096	774	4.32	84.4	48.5	9.10
Oct 2004 TP con	17	0	0.0134	0.0130	0.0145	0.897	6,213	754	4.33	85.8	49.4	9.48
Oct 2004 TP T1	17	24	0.0126	0.0158	0.0128	1.23	5,006	738	4.79	73.8	38.5	8.34
Oct 2004 TP T2	17	48	0.0119	0.0167	0.0124	1.34	4,624	687	4.93	70.1	35.1	8.51
Oct 2004 CBB init	26	0	0.0138	0.0196	0.0142	1.79	538	162	9.00	8.6	4.0	4.43
Oct 2004 CBB con	26	0	0.0116	0.0251	0.0104	2.52	558	174	6.17	8.6	4.0	4.15
Oct 2004 CBB T1	26	24	No data	No data	No data	No data	No data	174	No data	No data	No data	No data
Oct 2004 CBB T2	26	48	No data	No data	No data	No data	No data	164	No data	No data	No data	No data
May 2005 GB init	8	0	0.0148	0.0142	0.0188	0.760	6,693	929	5.06	92.9	51.5	8.34
May 2005 GB con	8	0	0.0147	0.0143	0.0190	0.755	6,732	896	4.98	92.9	51.7	8.65
May 2005 GB T1	8	24	0.0157	0.0170	0.0181	0.939	5,651	913	5.60	83.3	42.3	7.61
May 2005 GB T2	8	48	0.0166	0.0185	0.0185	0.997	4,819	852	6.12	74.7	35.5	7.31
May 2005 TP init	18	0	0.0164	0.0141	0.0158	0.888	4,461	623	4.96	60.6	33.9	8.11
May 2005 TP con	18	0	0.0161	0.0137	0.0145	0.948	4,595	538	4.89	61.5	34.7	9.54
May 2005 TP T1	18	24	0.0158	0.0171	0.0124	1.38	3,753	426	5.67	54.3	27.5	10.60
May 2005 TP T2	18	48	0.0168	0.0193	0.0127	1.52	3,021	514	6.71	47.5	21.7	7.71
May 2005 CBB init	25	0	0.0204	0.0227	0.0265	1.020	505	162	10.14	9.0	3.8	4.66
May 2005 CBB con	25	0	0.0192	0.0220	0.0214	0.996	558	174	7.82	9.4	4.0	4.51
May 2005 CBB T1	25	24	0.0208	0.0309	0.0315	1.24	350	No data	14.36	7.6	2.3	No data
May 2005 CBB T2	25	48	0.0211	0.0361	0.0306	1.87	261	176	26.89	6.7	1.6	3.17
Oct 2005 GB init	11	0	0.0154	0.0137	0.0166	0.824	8,418	No data	4.79	113.1	64.1	No data
Oct 2005 GB con	11	0	0.0156	0.0137	0.0169	0.813	8,277	No data	4.85	111.8	63.2	No data
Oct 2005 GB T1	11	24	0.0149	0.0156	0.0152	1.02	7,499	No data	5.12	104.9	55.8	No data
Oct 2005 GB T2	11	48	0.0142	0.0163	0.0144	1.13	7,077	No data	5.09	99.3	51.7	No data
Oct 2005 TP init	18	0	0.0156	0.0143	0.0168	0.850	4,479	No data	4.96	61.5	33.9	No data
Oct 2005 TP con	18	0	0.0156	0.0142	0.0167	0.850	4,484	No data	4.94	61.4	33.9	No data
Oct 2005 TP T1	18	24	0.0150	0.0171	0.0149	1.15	3,741	No data	5.53	54.5	27.4	No data
Oct 2005 TP T2	18	48	0.0159	0.0195	0.0155	1.26	2,997	No data	6.56	47.5	21.6	No data
Oct 2005 CBB init	23	0	0.0195	0.0221	0.0184	1.20	591	No data	8.85	10.1	4.3	No data

Table 2. Continued.

Sample name	Salinity	Irr <i>t</i> (h)	$S_{300-700}$ (nm ⁻¹)	$S_{275-295}$ (nm ⁻¹)	$S_{350-400}$ (nm ⁻¹)	S_R	Total <i>a</i> (250–450 nm)	DOC (mmol L ⁻¹)	$E_2 : E_3$	a_{254} (m ⁻¹)	a_{300} (m ⁻¹)	SUVA 254 (mg C L ⁻¹ m ⁻¹)
Oct 2005 CBB con	23	0	0.0181	0.0217	0.0187	1.16	594	No data	8.15	10.0	4.3	No data
Oct 2005 CBB T1	23	24	0.0173	0.0265	0.0144	1.84	461	No data	10.18	8.6	3.1	No data
Oct 2005 CBB T2	23	48	0.0168	0.0290	0.0141	2.06	390	No data	11.39	7.8	2.5	No data
Feb 2006 DS ox con	0	0	0.0158	0.0131	0.0186	0.70	65,471	No data	4.64	908.1	520.5	No data
Feb 2006 DS ox T1	0	144	0.0145	0.0170	0.0158	1.07	38,975	No data	4.97	554.5	275.3	No data
Feb 2006 DS anox con	0	0	0.0155	0.0131	0.0180	0.72	67,702	No data	4.57	900.7	518.2	No data
Feb 2006 DS anox T1	0	144	0.0149	0.0153	0.0170	1.11	57,258	No data	4.71	786.5	421.5	No data

magnitude and direction to those observed along the estuary (Fig. 7B,D). The change in absorption observed during photobleaching was considerably smaller than observed along the estuary, but does not incorporate mixing of low-absorbing water as occurs in the estuary. It is interesting to note that the duration of this experiment is considerably shorter than the freshwater residence time (~3.3 months) in the Delaware estuary (Dettmann 2001). We can therefore qualitatively attribute a considerable role in the spectral alteration of CDOM to photochemical degradation. This result is similar to those from more quantitative modeling studies for temperate UK estuaries, where photobleaching within the estuaries was estimated to account for up to 90% of the observed spectral slope shift from the head to the mouth (Stubbins 2001). The Delaware Estuary results in Fig. 8 show a strong influence from mixing, but the Stubbins result and our results shown in Fig. 7B,D raise an interesting question of whether marine DOM S and S_R are higher because the source is different or because river DOM is substantially photobleached during its transit to the ocean.

Coastal ocean transects—Near-surface (~2 m) measurements of S_R were 1.3 at the mouth of the Delaware Bay (38.86°N, 75.09°W), 1.5 at the shelf break (38.71°N, 73.77°W), 3.9 midway across the continental slope (40.12°N, 70.60°W), and 9.4 in the Sargasso Sea (36.43°N, 71.41°W). Comparing two locations in the GAB (Table 4), the near-shore site (about 50 km off the coast; 32.17°N, 79.99°W) showed average S_R values of 1.7 (± 0.1 ; $n = 6$) in surface water samples in summer 2003. Farther offshore, near the shelf break (about 140 km offshore; 31.76°N, 79.28°W), S_R values in surface waters averaged 4.6 (± 0.1 ; $n = 2$). The markedly higher S_R values measured at the offshore site are consistent with our measurements in the Sargasso Sea (Helms 2006) and with irradiation experiments.

Irradiation of the near-shore GAB sample (Sta. B) by either natural sunlight or a solar simulator resulted in an increase in $S_{275-295}$, S_R , and $E_2 : E_3$ and a decrease in $S_{350-400}$, $S_{300-700}$, a_{254} , a_{300} , and $E_4 : E_6$, whereas no changes were observed in the dark control. These photochemically induced shifts in the spectral parameters for the near-shore sample resulted in water with spectral properties approaching those of the offshore samples (Sta. C) (Tables 4, 5). The changes in spectral parameters are consistent with those obtained for the irradiated Elizabeth River and Chesapeake Bay samples, which showed that $S_{275-295}$ values increased, $S_{350-400}$ values decreased, S_R and $E_2 : E_3$ increased, and UV-visible absorption decreased upon irradiation. In addition, irradiation of terrestrially dominated low-salinity samples resulted in CDOM with optical properties characteristic of the nonirradiated marine-dominated high-salinity samples (Fig. 3; Tables 2, 5).

Discussion

Comparison of the UF data and CDOM a spectra obtained from Elizabeth River and Chesapeake Bay samples showed that $S_{275-295}$ and S_R are inversely related

Table 3. Spectral slope (*S*), total absorbance (*a*), and dissolved organic carbon (DOC) measured for each ultrafiltration size fraction of the Chesapeake Bay Bridge (CBB), Town Point (TP), Great Bridge (GB), and Dismal Swamp (DS); init=initial; con=dark control; T1=irradiated 24 h; T2=48 h.

Sample name	Salinity	Irr t (h)	UF filtrate				UF retentate					
			<i>S</i> ₂₇₅₋₂₉₅ (nm ⁻¹)	<i>S</i> ₃₅₀₋₄₀₀ (nm ⁻¹)	<i>S_R</i>	Total <i>a</i> (250-450 nm)	DOC (mmol L ⁻¹)	<i>S</i> ₂₇₅₋₂₉₅ (nm ⁻¹)	<i>S</i> ₃₅₀₋₄₀₀ (nm ⁻¹)	<i>S_R</i>	Total <i>a</i> (250-450 nm) volume corrected	DOC volume corrected (mmol L ⁻¹)
May 2004 GB init	12	0	0.0188	0.0208	0.904	1.339	342	0.0133	0.0163	0.818	5,168	559
May 2004 GB con	12	0	0.0190	0.0206	0.920	1,184	336	0.0133	0.0163	0.813	5,343	608
May 2004 GB T1	12	24	0.0205	0.0195	1.05	1,368	351	0.0147	0.0149	0.983	4,348	521
May 2004 GB T2	12	48	0.0279	0.0144	0.988	1,155	287	0.0156	0.0149	1.05	3,417	497
May 2004 TP init	19	0	0.0175	0.0177	0.988	944	213	0.0129	0.0155	0.828	2,143	264
May 2004 TP con	19	0	0.0165	0.0165	1.00	789	177	0.0129	0.0157	0.822	2,032	229
May 2004 TP T1	19	24	0.0246	0.0154	1.60	887	251	0.0158	0.0143	1.11	1,609	249
May 2004 TP T2	19	48	0.0274	0.0156	1.76	848	243	0.0167	0.0143	1.17	1,072	213
May 2004 CBB init	23	0	0.0221	0.0312	0.708	311	113	0.0190	0.0166	1.14	238	74
May 2004 CBB con	23	0	0.0180	0.0292	0.615	253	105	0.0194	0.0164	1.18	262	90
May 2004 CBB T1	23	24	0.0278	0.0169	1.65	261	119	0.0222	0.0159	1.40	177	85
May 2004 CBB T2	23	48	0.0263	0.0021	12.8	189	115	0.0254	0.0166	1.53	128	80
Oct 2004 GB init	10	0	0.0128	0.0128	1.08	1,762	333	0.0123	0.0153	0.802	9,147	865
Oct 2004 GB con	10	0	0.0148	0.0129	1.14	2,066	383	0.0123	0.0153	0.807	8,239	857
Oct 2004 GB T1	10	24	0.0172	0.0129	1.34	2,764	638	0.0135	0.0137	0.988	7,169	654
Oct 2004 GB T2	10	48	0.0196	0.0116	1.69	2,106	409	0.0150	0.0142	1.06	5,980	720
Oct 2004 TP init	17	0	0.0134	0.0125	1.07	1,482	279	0.0125	0.0150	0.830	4,324	458
Oct 2004 TP con	17	0	0.0148	0.0134	1.11	1,516	292	0.0122	0.0145	0.839	4,896	469
Oct 2004 TP T1	17	24	0.0187	0.0115	1.63	1,615	274	0.0140	0.0135	1.04	3,398	386
Oct 2004 TP T2	17	48	0.0211	0.0115	1.83	1,464	337	0.0154	0.0135	1.15	2,670	323
Oct 2004 CBB init	26	0	0.0255	0.0249	1.02	334	143	0.0205	0.0176	1.17	153	57
Oct 2004 CBB con	26	0	0.0192	0.0230	0.834	283	116	0.0199	0.0147	1.35	122	36
Oct 2004 CBB T1	26	24	No data	No data	No data	No data	107	No data	No data	No data	No data	48
Oct 2004 CBB T2	26	48	No data	No data	No data	No data	136	No data	No data	No data	No data	39
May 2005 GB init	8	0	0.0159	0.0200	0.795	1,795	376	0.0161	0.0150	1.07	4,396	562
May 2005 GB con	8	0	0.0235	0.0170	1.38	1,958	387	0.0155	0.0154	1.00	4,403	568
May 2005 GB T1	8	24	0.0166	0.0186	0.889	1,676	607	0.0133	0.0168	0.789	4,515	512
May 2005 GB T2	8	48	0.0212	0.0111	1.90	1,556	392	0.0132	0.0165	0.801	2,829	409
May 2005 TP init	18	0	0.0183	0.0214	0.856	1,005	226	0.0130	0.0166	0.783	3,185	320
May 2005 TP con	18	0	0.0224	0.0183	1.22	1,132	244	0.0170	0.0169	1.00	3,383	327
May 2005 TP T1	18	24	0.0173	0.0173	0.997	1,385	257	0.0130	0.0161	0.809	2,084	220
May 2005 TP T2	18	48	0.0207	0.0164	1.23	1,162	533	0.0147	0.0150	0.980	1,904	236
May 2005 CBB init	25	0	0.0233	0.0209	1.12	232	90	No data	No data	No data	No data	37
May 2005 CBB con	25	0	0.0234	0.0220	1.07	256	91	No data	No data	No data	No data	36
May 2005 CBB T1	25	24	0.0283	0.0165	1.71	153	No data	No data	No data	No data	No data	No data
May 2005 CBB T2	25	48	0.0295	0.0183	1.62	117	113.8	No data	No data	No data	No data	32
Oct 2005 GB init	11	0	0.0169	0.0211	0.801	1,620	No data	0.0130	0.0167	0.778	6,025	No data
Oct 2005 GB con	11	0	0.0167	0.0210	0.795	1,777	No data	0.0130	0.0167	0.778	6,056	No data
Oct 2005 GB T1	11	24	0.0195	0.0183	1.06	1,899	No data	0.0145	0.0153	0.948	5,021	No data
Oct 2005 GB T2	11	48	0.0211	0.0190	1.11	1,953	No data	0.0152	0.0151	1.01	4,301	No data
Oct 2005 TP init	18	0	0.0174	0.0197	0.883	1,047	No data	0.0132	0.0168	0.786	3,015	No data
Oct 2005 TP con	18	0	0.0176	0.0206	0.854	1,052	No data	0.0133	0.0170	0.782	2,780	No data
Oct 2005 TP T1	18	24	0.0220	0.0196	1.12	1,063	No data	0.0160	0.0153	1.05	2,388	No data

Table 3. Continued.

Sample name	Salinity	Irr t (h)	UF filtrate					UF retentate				
			$S_{275-295}$ (nm^{-1})	$S_{350-400}$ (nm^{-1})	S_R	Total a (250–450 nm)	DOC (mmol L^{-1})	$S_{275-295}$ (nm^{-1})	$S_{350-400}$ (nm^{-1})	S_R	Total a (250–450 nm) volume corrected	DOC volume corrected (mmol L^{-1})
Oct 2005 TP T2	18	48	0.0241	0.0183	1.32	1,024	No data	0.0177	0.0162	1.09	1,658	No data
Oct 2005 CBB init	23	0	0.0224	0.0190	1.18	292	No data	0.0206	0.0185	1.11	323	No data
Oct 2005 CBB con	23	0	0.0229	0.0203	1.13	402	No data	0.0187	0.0171	1.09	189	No data
Oct 2005 CBB T1	23	24	0.0274	0.0197	1.39	278	No data	0.0243	0.0146	1.66	187	No data
Oct 2005 CBB T2	23	48	0.0286	0.0135	2.12	266	No data	0.0270	0.0157	1.72	146	No data
Feb 2006 DS ox	0	0	0.0180	0.0267	0.676	6,141	No data	0.0127	0.0172	0.739	58,074	No data
Feb 2006 DS ox T1	0	144	0.0209	0.0206	1.01	9,466	No data	0.0142	0.0135	1.05	30,134	No data
Feb 2006 DS anox	0	0	0.0178	0.0252	0.706	5,073	No data	0.0128	0.0174	0.735	59,603	No data
Feb 2006 DS anox T1	0	144	0.0193	0.0200	0.963	6,858	No data	0.0138	0.0150	0.924	49,031	No data

to the MW of the CDOM in a water sample. A similar trend was also observed for SRNOM that was fractionated by GFC. Using flow field–flow fractionation, Fløge and Wells (2007) demonstrated that the spectral shape covaried with size for colloidal CDOM. That these relationships are observed over a broad and continuous MW range of size-fractionated natural organic matter samples indicates that variations in spectral shape parameters with MW have a physicochemical basis. The above results, plus the fact that DOC-based MWs generally reflect the CDOM-based MWs (Fig. 4), indicate that UV spectral slopes have considerable potential for semiquantitative assessment of DOM MW. However, further research is needed to determine whether such relationships between S_R and average MW are system dependent or more widely applicable.

Our UF data clearly indicate that spectral shifts in S and S_R are accompanied by variations in both DOC and CDOM MW (e.g., Fig. 4, Tables 2, 3, 5). The decrease in CDOM MW with irradiation implies that chromophores associated with HMW CDOM are destroyed during photobleaching, resulting in a significant portion of the CDOM shifting from the HMW pool to the LMW pool (e.g., due to bond cleavage or disaggregation [or both]). These results are consistent with but cannot distinguish between the two current conceptual models for CDOM spectral shape, i.e., a polydispersed mixture of discrete chromophores versus intramolecular charge transfer. If CDOM behaves as a polydispersed mixture of conjugated organic chromophores, then the LMW material should absorb shorter-wavelength radiation (Pavia et al. 1979); therefore, when the MW distribution is shifted to lower MW by photodegradation, the shape of the absorption spectrum should shift to greater relative absorption at shorter wavelengths. On the other hand, if the primary factor controlling CDOM optical properties is the intramolecular charge transfer capability of CDOM (Del Vecchio and Blough 2004b), then a decrease in MW would alter (and probably diminish) the potential for intramolecular charge transfer interactions, which again would shift the absorption spectrum toward shorter wavelengths, causing steeper $S_{275-295}$, shallower $S_{350-400}$, and increased S_R .

The large change in the spectral shape during irradiation of Dismal Swamp water at low oxygen levels (4% larger increase in S_R in the low-oxygen sample) concomitant with a smaller shift in MW (70% smaller increase in %LMW in the low-oxygen sample) than occurred during air-saturated irradiations (Table 2) suggests that (1) the CDOM charge transfer system (Del Vecchio and Blough 2004b) was significantly altered by photochemical reactions, even at low oxygen concentrations, and (2) oxidative cleavage of covalent bonds, probably by reactive oxygen species (Andrews et al. 2000), appears to be more impeded under suboxic conditions than the disruption of DOM donor–acceptor charge transfer groups. Thus the decoupling of MW, S , and S_R in this experiment is more consistent with the charge transfer model. Further study of the wavelength dependence of spectral slope shifts and the compositional changes accompanying these photochemically induced shifts is clearly needed.

Estuarine changes in spectra resulted in increases in S_R by nearly a factor of two between the DOM-rich terrestrial

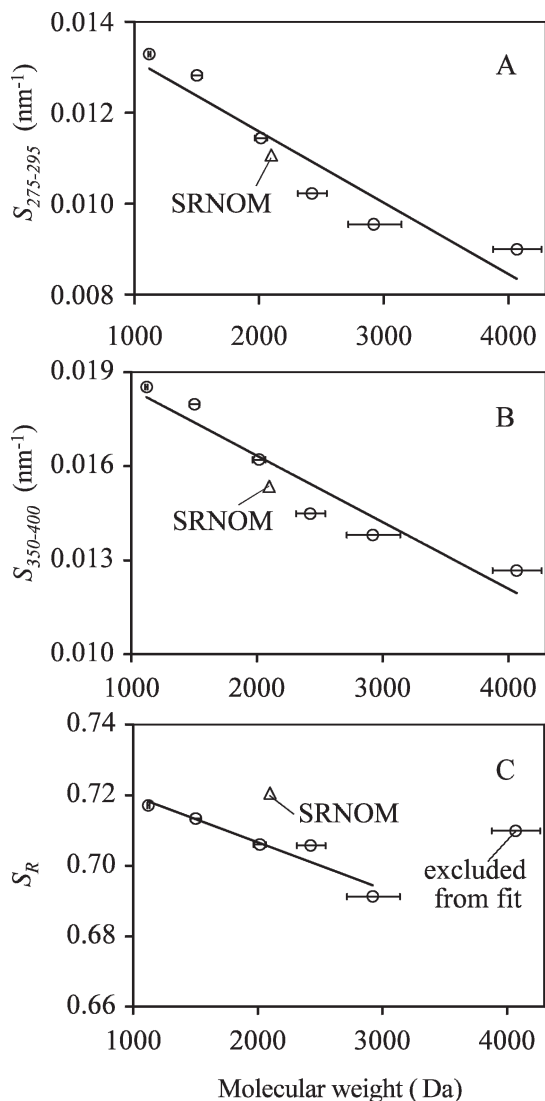


Fig. 5. Regression plot of (A and B) spectral slopes and (C) ratio of spectral slopes, S_R , versus apparent MW (weight average) of size-fractionated Suwannee River natural organic matter (SRNOM) as determined by size exclusion chromatography. Horizontal bars represent standard deviation. The open triangle indicates the unfractiated SRNOM datum. (A) Slope = -1.57×10^{-6} , intercept = 0.0147, $r^2 = 0.896$; (B) slope = -2.12×10^{-6} , intercept = 0.0206, $r^2 = 0.9195$; (C) slope = -1.32×10^{-5} , intercept = 0.7331, $r^2 = 0.9141$.

freshwater end member and the surface waters from near the mouth of the Delaware Estuary. These shifts are probably related to changes in DOM molecular size and composition during transit through the estuary. In addition, CDOM spectral properties are affected by ionic strength and pH shifts during estuarine transit (Minor et al. 2006, unpubl. data). However, on the basis of previous photochemical modeling studies in other midlatitude estuaries (Stubbins 2001), the spectral changes that we observed in the Delaware were probably caused by photobleaching of DOM (e.g., photo-oxidative degradation), mixing, and, to a lesser extent, flocculation, microbial

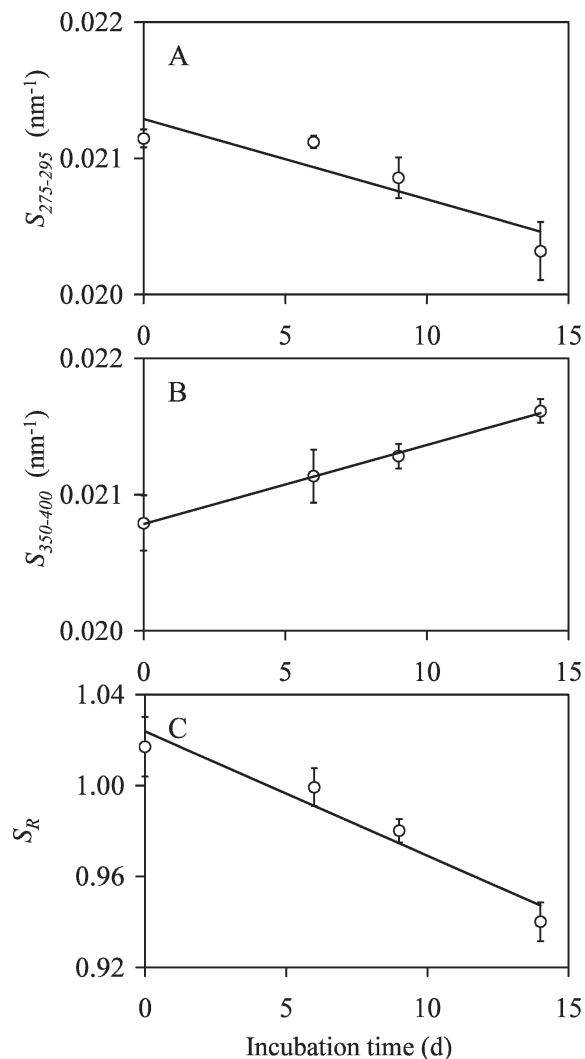


Fig. 6. Regression plot of (A and B) spectral slopes and (C) ratio of spectral slopes, S_R , versus incubation (aerobic) time of unfiltered Elizabeth River (ODU Sailing Basin) water. Error bars represent standard deviation from replicate subsamples ($n = 3$) that were poisoned and stored in separate vials. (A) Slope = -6.0×10^{-5} , intercept = 0.021, $r^2 = 0.807$; (B) slope = 6.0×10^{-5} , intercept = 0.021, $r^2 = 0.997$; (C) slope = -5.5×10^{-3} , intercept = 1.0, $r^2 = 0.940$.

alteration or production of CDOM, and inputs from marshes and sediments (especially in the bay). S_R is therefore a potentially useful integrative indicator of CDOM history (source and transformations) in natural waters.

The ratio of spectral slopes (S_R) is a fast and reproducible method for characterizing CDOM in natural waters. Spectral corrections and calculations used to obtain S_R are considerably simpler than those needed to determine excitation–emission matrices (EEMs). Furthermore, S_R values can be measured across diverse aquatic regimes (e.g., from the black waters of the Great Dismal Swamp to highly photobleached Sargasso Sea surface waters) and provide strong differentiation between open ocean, coastal

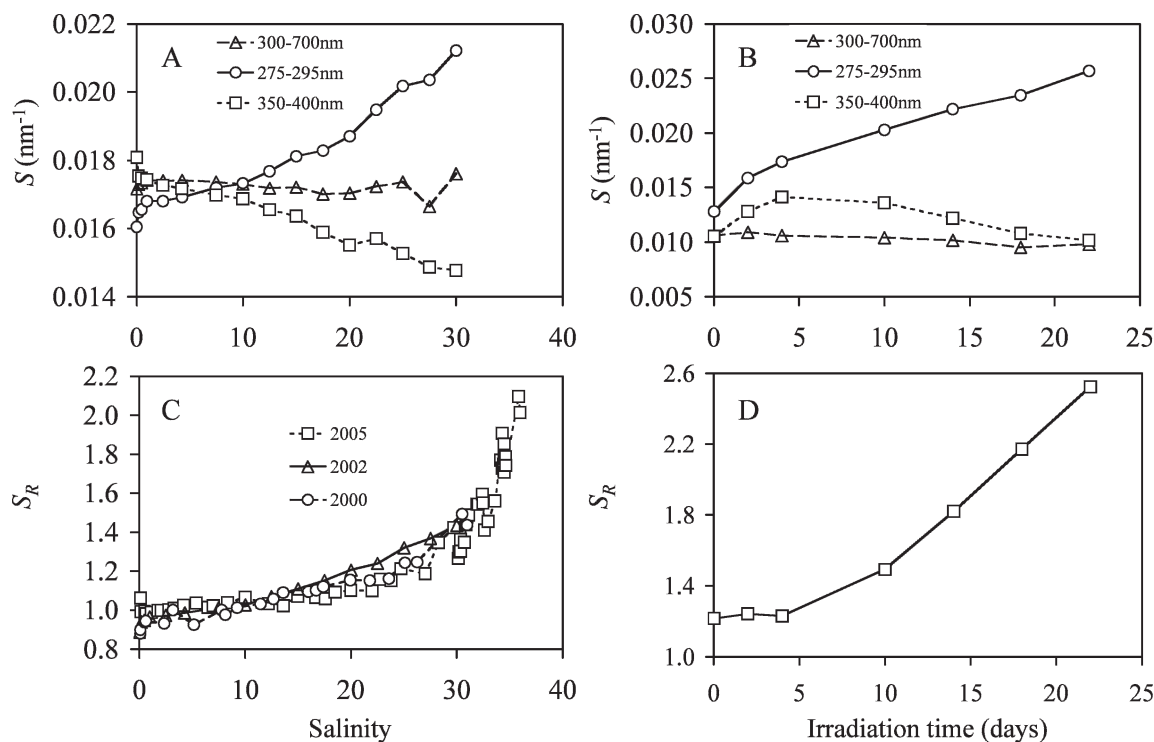


Fig. 7. Spectral parameters measured within the Delaware Estuary and in rooftop-irradiated samples of Delaware River water (Yardley, Pennsylvania Public Boat Ramp, 80 liters, summer 2006): (A) spectral slope coefficients along the estuary (summer 2002) and (B) in irradiated river sample, (C) ratio of spectral slopes, S_R (summer 2000, 2002, and 2005), and (D) in irradiated river sample.

ocean, estuarine, and riverine surface waters. For example, between the Delaware River and the Sargasso Sea, S_R varies by more than a factor of 11 (and by over a factor of 13 between DOM-rich Dismal Swamp water and Sargasso Sea surface water). The S_R term, because of its independence from DOC concentration, may therefore be useful for differentiating open ocean waters from those of near-shore coastal or estuarine origin.

A potentially important application of S_R is in the analysis of ballast water. To limit the proliferation of invasive aquatic species (Choi et al. 2005), seafaring vessels are required to exchange their ballast water at least 200 miles from shore (Murphy et al. 2003). Our spectral analysis provides a rapid analytical tool for differentiating inland waters from oceanic regimes with considerable accuracy and reproducibility, and it may be a simple alternative or supplement to using EEMs. However, further research is needed to determine whether our approach is robust enough to be effective in an environment likely to contain large amounts of petroleum and metal contamination. Other potential applications for the two-slope approach include detecting zones of enhanced microbial heterotrophy and tracing recently subducted, photobleached surface water, e.g., 18° subtropical-mode water formation (Helms 2006).

A consistent set of definitions for describing the shape and wavelength ranges of log-transformed CDOM spectra is clearly needed to facilitate comparison of field data and

experimental results in the literature. Currently, no consensus exists. In this study, we have identified two linear wavelength regions that appear applicable to a wide variety of water types, including DOM-rich terrestrial water, estuarine waters, coastal waters, and highly photobleached, DOM-poor open oceanic water, as well as size-fractionated samples. Reliable measurement of absorption at wavelengths longer than ~ 400 nm are problematic for many instruments. Several approaches have been used to deal with this problem when calculating CDOM spectral slopes in the visible region. The use of variable wavelength cutoffs has resulted in data that are very difficult to compare (Twardowski et al. 2004). The use of nonlinear regression to calculate $S_{300-700}$ has improved this situation. However, it requires considerably more computing power and data processing than our approach for calculating $S_{350-400}$. The slope of the short wavelength range (275–295 nm), which can be measured with high precision (even in highly photobleached open ocean waters), appears to be particularly sensitive to, and perhaps also indicative of, shifts in MW or DOM sources (or both), whereas the use of broader wavelength ranges (e.g., several hundred nanometers), as is commonly practiced, is not sensitive enough to identify these shifts. Therefore, we strongly advocate the inclusion of this short wavelength slope in future DOM studies, as it would not only provide insights into DOM MW and source, but also greatly facilitate comparisons among investigations and water types.

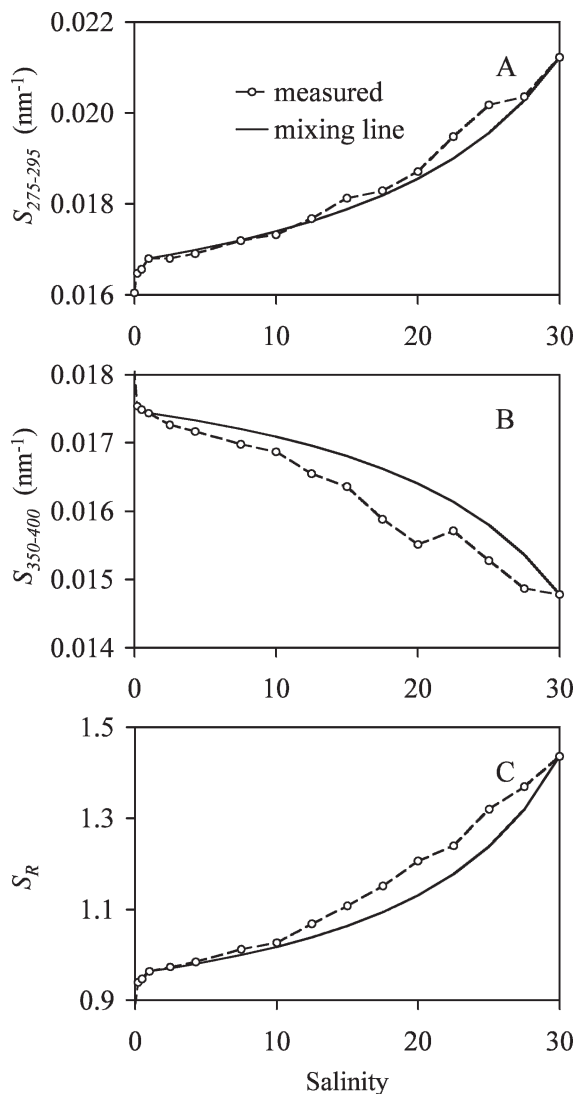


Fig. 8. Measured values and ideal mixing lines for (A) $S_{275-295}$, (B) $S_{350-400}$, and (C) S_R in the Delaware Estuary (summer 2002). Salinity = 1 was used for freshwater end member because of flocculation, particle adsorption, or apparent third end member at lower salinities.

Table 4. Average spectral parameters (± 1 SD) for two sites in the Georgia Bight (GAB; June 2003). For Sta. B, $n = 6$; for Sta. C, $n = 2$. Replicate measurements were from separate samples taken from the same station and depth.

	Nearshore GAB(B)	Offshore GAB(C)
$S_{300-700}$ (nm^{-1})	0.0148 ± 0.0006	0.0086 ± 0.0009
$S_{275-295}$ (nm^{-1})	0.024 ± 0.002	0.036 ± 0.001
$S_{350-400}$ (nm^{-1})	0.0135 ± 0.0003	0.0078 ± 0.0001
S_R	1.74 ± 0.15	4.56 ± 0.13
$E_2 : E_3$	8.7 ± 1.4	13.5 ± 1.6
$E_4 : E_6$	4.63 ± 1.0	2.71 ± 1.0
a_{254} (m^{-1})	3.368 ± 0.001	1.78 ± 0.06
a_{300} (m^{-1})	1.33 ± 0.15	0.400 ± 0.034

Table 5. Spectral parameters of Georgia Bight (Sta. B) surface water samples altered by irradiation with natural and artificial sunlight.

	Dark control	8 h of natural sunlight	18 h of artificial sunlight
$S_{300-700}$ (nm^{-1})	0.0150	0.0132	0.0139
$S_{275-295}$ (nm^{-1})	0.025	0.028	0.032
$S_{350-400}$ (nm^{-1})	0.015	0.013	0.013
S_R	1.705	2.082	2.42
$E_2 : E_3$	8.621	8.967	11.2
$E_4 : E_6$	4.3	4.095	3.372
a_{254} (m^{-1})	3.24	3.228	2.913
a_{300} (m^{-1})	1.23	1.11	0.840

References

- ANDREWS, S. S., S. CARON, AND O. C. ZAFIRIOU. 2000. Photochemical oxygen consumption in marine waters: A major sink for colored dissolved organic matter? *Limnol. Oceanogr.* **45**: 267–277.
- BROWN, M. 1977. Transmission spectroscopy examinations of natural waters. *Estuar. Coast. Mar. Sci.* **5**: 309–317.
- CARDER, K. L. R. G., STEWARD, G. R. HARVEY, AND P. B. ORTNER. 1989. Marine humic and fulvic acids: Their effects on remote sensing of ocean chlorophyll. *Limnol. Oceanogr.* **34**: 68–81.
- CHEN, Y., N. SENESI, AND M. SCHNITZER. 1977. Information provided on humic substances by $E_4:E_6$ ratios. *Soil Sci. Soc. Am. J.* **41**: 352–358.
- CHIN, Y. P., G. AIKEN, AND E. O'LOUGHLIN. 1994. Molecular weight, polydispersity, and spectroscopic properties of aquatic humic substances. *Environ. Sci. Technol.* **26**: 1853–1858.
- CHOI, K. H., W. KIMMERER, G. SMITH, G. RUIZ, AND K. LION. 2005. Post-exchange zooplankton in ballast water of ships entering the San Francisco Estuary. *J. Plankton Res.* **27**: 707–714.
- DE HAAN, H., AND T. DE BOER. 1987. Applicability of light absorbance and fluorescence as measures of concentration and molecular size of dissolved organic carbon in humic Laken Tjeukemeer. *Water Res.* **21**: 731–734.
- DEL VECCHIO, R., AND N. V. BLOUGH. 2002. Photobleaching of chromophoric dissolved organic matter in natural waters: Kinetics and modeling. *Mar. Chem.* **78**: 231–253.
- , AND ———. 2004a. Spatial and seasonal distribution of chromophoric dissolved organic matter and dissolved organic carbon in the Middle Atlantic Bight. *Mar. Chem.* **89**: 169–187.
- , AND ———. 2004b. On the origin of the optical properties of humic substances. *Environ. Sci. Technol.* **38**: 3885–3891.
- DETTMANN, E. H. 2001. Effect of water residence time on annual export and denitrification of nitrogen in estuaries: A model analysis. *Estuaries* **24**: 481–490.
- FLOGE, S. A., AND M. L. WELLS. 2007. Variation in colloidal chromophoric dissolved organic matter in the Damariscotta Estuary, Maine. *Limnol. Oceanogr.* **52**: 32–45.
- GAO, H. Z., AND R. G. ZEPP. 1998. Factors influencing photoreactions of dissolved organic matter in coastal river of the southern United States. *Environ. Sci. Technol.* **32**: 2940–2946.
- GREEN, S. A., AND N. V. BLOUGH. 1994. Optical absorption and fluorescence properties of chromophoric dissolved organic matter in natural waters. *Limnol. Oceanogr.* **39**: 1903–1916.

- HAYASE, K., AND H. TSUBOTA. 1985. Sedimentary humic-acid and fulvic-acid as fluorescent organic materials. *Geochim. Cosmochim. Acta* **49**: 159–163.
- HELMS, J. R. 2006. Spectral shape as an indicator of molecular weight in chromophoric dissolved organic matter. M.S. thesis, Old Dominion Univ.
- LEIFER, A. 1988. The kinetics of environmental aquatic photochemistry: Theory and practice. American Chemical Society.
- MILLER, W. L. 1994. Recent advances in the photochemistry of natural dissolved organic matter p. 111–128. *In* G. R. Helz, R. G. Zepp, and D. G. Crosby [eds.], *Aquatic and surface photochemistry*. CRC Press.
- MINOR, E. C., J. POTHEN, B. J. DALZELL, H. ABDULLA, AND K. MOPPER. 2006. Effects of salinity changes on the photodegradation and UV-visible absorbance of terrestrial dissolved organic matter. *Limnol. Oceanogr.* **51**: 2181–2186.
- MOPPER, K., AND D. J. KIEBER. 2002. Photochemistry and the cycling of carbon, sulfur, nitrogen and phosphorus p. 455–489. *In* D. Hansell and C. Carlson [eds.], *Biogeochemistry of marine organic matter*. Academic Press.
- MORAN, M. A., W. M. SHELDON, JR., AND R. G. ZEPP. 2000. Carbon loss and optical property changes during long-term photochemical and biological degradation of estuarine organic matter. *Limnol. Oceanogr.* **45**: 1254–1264.
- MORRIS, D. P., AND B. R. HARGRAEVES. 1997. The role of photochemical degradation of dissolved organic carbon in regulating the UV transparency of three lakes on the Pocono Plateau. *Limnol. Oceanogr.* **42**: 239–249.
- MURPHY, K., AND OTHERS. 2003. Verification of mid-ocean ballast water exchanging using naturally occurring coastal tracers. *Mar. Poll. Bull.* **48**: 711–730.
- PAVIA, D. L., G. M. LAMPMAN, AND G. S. KRIZ. 1979. *Introduction to spectroscopy: A guide for students of organic chemistry*. Saunders.
- PEURAVOURI, J., AND K. PIHLAJA. 1997. Molecular size distribution and spectroscopic properties of aquatic humic substances. *Anal. Chim. Acta* **337**: 133–149.
- PICCOLO, A., P. ZACCHEO, AND P. G. GENEVINI. 1992. Chemical characterization of humic substances extracted from organic-waste-amended soils. *Biores. Technol.* **40**: 275–282.
- RITCHIE, J. D. 2005. The distribution of charge and acidic functional groups in the Suwannee River natural organic matter: The dependence on molecular weight and pH. Ph.D. thesis, Georgia Institute of Technology.
- SARPAL, R. S., K. MOPPER, AND D. J. KEIBER. 1995. Absorbance properties of dissolved organic matter in Antarctic sea water. *Antarc. J.* **30**: 139–140.
- SCHMIT, K. H., AND M. J. M. WELLS. 2002. Preferential adsorption of fluorescing fulvic and humic acid components on activated carbon using flow field-flow fractionation analysis. *J. Environ. Monit.* **4**: 75–84.
- SCHWARZ, J. N., AND OTHERS. 2002. Two models for absorption by coloured dissolved organic matter (CDOM). *Oceanologia* **44**: 209–241.
- SENESE, N., T. M. MIANO, M. R. PROVENZANO, AND G. BRUNETTI. 1989. Spectroscopic and compositional comparative characterization of I.H.S.S. reference and standard fulvic and humic acids of various origin. *Sci. Tot. Environ.* **81/82**: 143–156.
- STEDMON, C. A., S. MARKAGER, AND H. KAAS. 2000. Optical properties and signatures of chromophoric dissolved organic matter (CDOM) in Danish coastal waters. *Estuar. Coast. Shelf Sci.* **51**: 267–278.
- STUBBINS, A. P. 2001. Aspects of aquatic CO photoproduction from CDOM. Ph.D. thesis, New Castle Upon Tyne Univ.
- . 2006. Open-ocean carbon monoxide photoproduction. *Deep Sea Res. II.* **53**: 1695–1705.
- SUMMERS, R. S., P. K. CORNEL, AND P. V. ROBERTS. 1987. Molecular size distribution and spectroscopic characterization of humic substances. *Sci. Tot. Environ.* **62**: 27–37.
- TWARDOWSKI, M. S., E. BOSS, J. M. SULLIVAN, AND P. L. DONAGHAY. 2004. Modeling the spectral shape of absorbing chromophoric dissolved organic matter. *Mar. Chem.* **89**: 69–88.
- VÄHÄTALO, A. V., AND R. G. WETZEL. 2004. Photochemical and microbial decomposition of chromophoric dissolved organic matter during long (months-years) exposures. *Mar. Chem.* **89**: 313–326.
- WALSH, J. J., AND OTHERS. 2003. Phytoplankton response to intrusions of slope water on the West Florida Shelf: Models and observations. *J. Geophys. Res. Oceans* **108**: 21–31.
- WEISHAAR, J. L., G. R. AIKEN, B. A. BERGAMASCHI, M. S. FRAM, R. FUGII, AND K. MOPPER. 2003. Evaluation of specific ultraviolet absorbance as an indicator of the chemical composition and reactivity of dissolved organic carbon. *Environ. Sci. Technol.* **37**: 4702–4708.
- WHITEHEAD, R. F., S. DE MORA, S. DEMERS, M. GOSSELIN, P. MONFORT, AND B. MOSTAJIR. 2000. Interactions of ultraviolet-B radiation, mixing, and biological activity on photobleaching of natural chromophoric dissolved organic matter: A mesocosm study. *Limnol. Oceanogr.* **45**: 278–291.
- ZEPP, R. G., AND P. F. SCHLOTZHAUER. 1981. Comparison of photochemical behavior of various humic substances in water: 3. Spectroscopic properties of humic substances. *Chemosphere* **10**: 479–486.

Received: 14 May 2007
Accepted: 22 December 2007
Amended: 7 January 2008